

# Preliminary Comparison of Classifiers to Detect Spatio-spectral Patterns of Epileptic Seizures via PARAFAC Decomposition

Marlis Ontivero-Ortega, Yalina García-Puente and Eduardo Martínez-Montes  
*Cuban Neuroscience Center, Havana, Cuba*

## 1 OBJECTIVES

The automatic detection of epileptic seizures from EEG recording is very important for clinical diagnosis and monitoring and has become an issue of major scientific and technological interest (Orosco et al., 2013). In this work, we use the spatio-spectral features extracted via multi-dimensional Parallel Factor (PARAFAC) Analysis of the EEG for seizure detection. This subject-specific approach only requires extracting one component that explains a seizure's space-time-frequency pattern. Then, a simple adaptive zero-training technique (AZT) to classify the seizures, with the additional advantages of being fast and work online, is evaluated and compared with known pattern recognition methodologies (LDA, SVM, k-Means), according to its accuracy, sensitivity and specificity on EEG recordings of two epileptic paediatric patients.

## 2 METHODS

Two epileptic paediatric EEG data are used for seizure detection. The first one (0.5h, 19 channels, sampling frequency of 200Hz) corresponds to a patient of the Center for Neurological Restoration, at Havana ([www.ciren.cu](http://www.ciren.cu)), while the second (4h, 23 channels, sampling frequency of 256Hz) corresponds to patient chb01 of the epilepsy CHB-MIT scalp EEG database, available online at <http://www.physionet.org/pn6/chbmit>.

### 2.1 PARAFAC Model

The PARAFAC model is a multidimensional generalization of the Principal Component Analysis, with the advantage that the multilinear decomposition is unique under very mild conditions, without imposing orthogonality or statistical independence among components (Miwakeichi et al., 2004). In our case, the spectrograms of every

channel of an EEG segment are arranged into a 3D array, indexed by time, frequency and electrodes (spatial dimension). PARAFAC decomposes this tensor into components, each with corresponding temporal, spectral and spatial signatures (Miwakeichi et al., 2004). The spatial and spectral signatures obtained from PARAFAC analysis of a pattern epileptic seizure, can be used for searching these characteristics in new EEG segments. As the epileptic activity can be explained by one or more components, it is important to choose the component better explaining the epileptic activity to be detected. In this work, we explore the option of taking the first component of PARAFAC "blindly", which allows for a faster and more automatic procedure. EEG spectrograms and features (mean power ratio) were found following the same procedure as in (Martínez-Montes et al., 2013). This was done for the same data sets using different segments' length to test for the effect of this practical parameter which defines speed and computational load of the methodology. Table 1 summarizes the data used.

Table 1: Number of seizure and non-seizure segments, for different segments' length.

| Data | Length =     | 2 s     | 4 s     | 6 s     | 10 s    |
|------|--------------|---------|---------|---------|---------|
| 1    | Seiz/NonSeiz | 30/957  | 19/475  | 14/315  | 11/187  |
|      | Total        | 987     | 494     | 329     | 198     |
| 2    | Seiz/NonSeiz | 80/7120 | 42/3558 | 29/2371 | 19/1421 |
|      | Total        | 7200    | 3600    | 2400    | 1440    |

### 2.2 Seizure Detection

LDA and SVM classifiers were used (10-fold cross-validation) to detect seizures offline from the features of all segments, using every seizure segment as the pattern. In addition an ad-hoc binary threshold (mean power ratio of 0.5) and k-means clustering were used for comparison purposes. We also introduce a simple adaptive zero-training technique (AZT), based in the online classification of each segment by computing the probability to belong to two normal distributions that define the

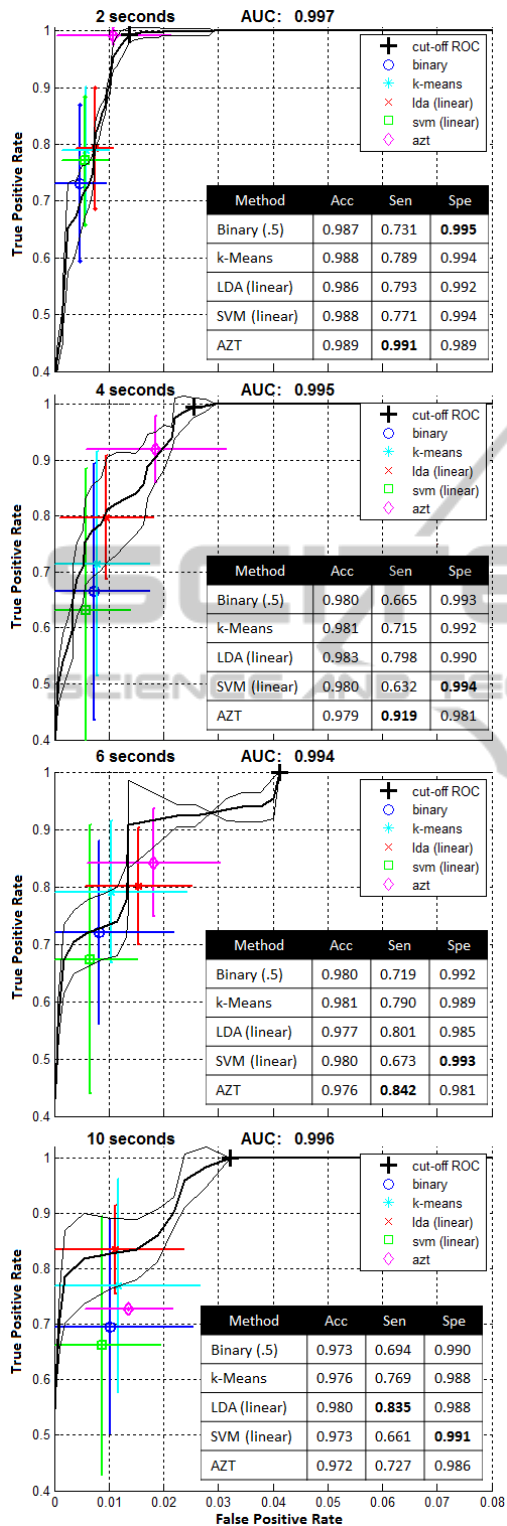


Figure 1: Data 1 - Mean (thick) and Standard deviation (thin) ROC curves for the mean power ratio. For the 5 classifiers the Mean and false/true positive rate Std bars for automatic thresholds are shown. The tables show the average Mean accuracy, sensitivity and specificity.

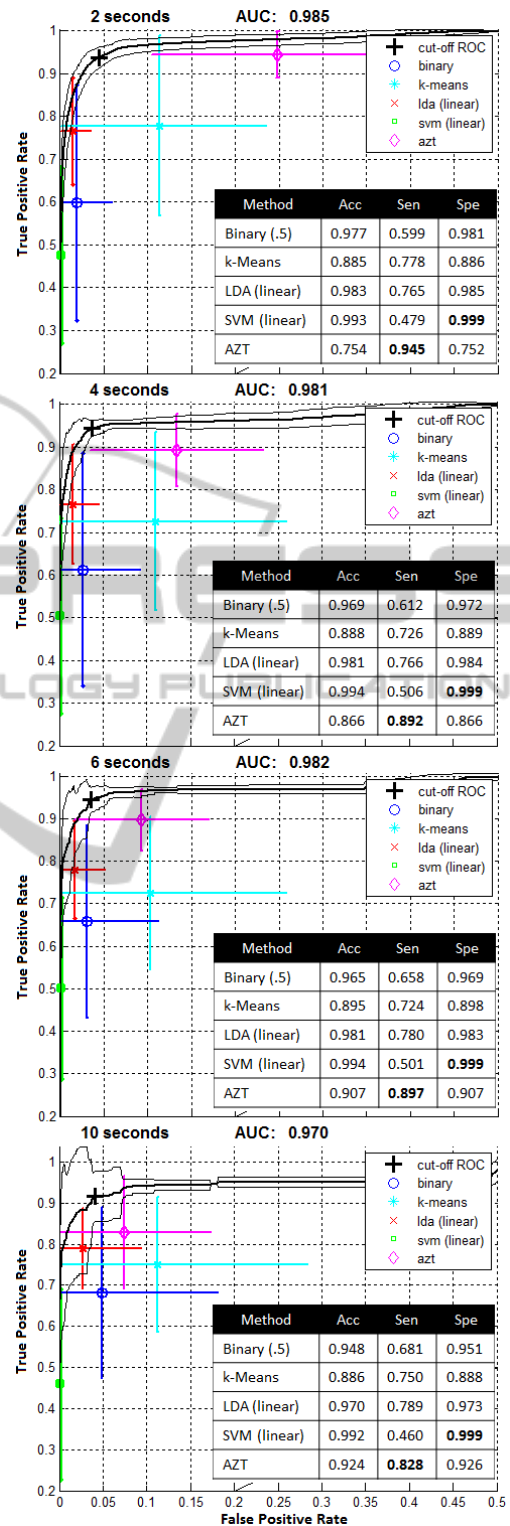


Figure 2: Data 2 - Mean (thick) and Standard deviation (thin) ROC curves for the mean power ratio. For the 5 classifiers the Mean and false/true positive rate Std bars for automatic thresholds are shown. The tables show the average Mean accuracy, sensitivity and specificity.

seizure and non-seizure classes. Initial means and standard deviations are fixed to [1, 1] (seizure) and [0, 0.5] (non-seizure), then they are iteratively updated for an adaptive classification.

### 3 RESULTS

ROC curves (true positives vs. false positives), area under the curve (AUC), automatic thresholds and classification results (accuracy, sensitivity, specificity in tables) are shown in figures 1 and 2. In both figures, a region is plotted (zoom) for better visualizing the behaviour of automatic thresholds.

The mean and standard deviation of ROCs (across all segments used as the pattern) for segment's length of 2, 4, 6 and 10 seconds; together with the optimal cut-off point (nearest point to (0, 1)) confirm the high potential of this feature for detection purposes.

Table 2 shows a quantitative comparison of the goodness of the automatic thresholds derived from the classifiers, as measured by the Euclidean distance between their sensitivity/specificity and those of the best cut-off of the ROC for all seizure patterns and different segments' length.

Table 2: Mean  $\pm$  Std of Euclidean distances between optimal cut-off and automatic thresholds.

|        | Method  | 2 s                             | 4 s                             | 6 s                             | 10 s                            |
|--------|---------|---------------------------------|---------------------------------|---------------------------------|---------------------------------|
| Data 1 | Binary  | 0.27 $\pm$ 0.14                 | 0.34 $\pm$ 0.23                 | 0.28 $\pm$ 0.16                 | 0.31 $\pm$ 0.19                 |
|        | k-Means | 0.21 $\pm$ 0.11                 | 0.29 $\pm$ 0.20                 | 0.21 $\pm$ 0.12                 | 0.23 $\pm$ 0.19                 |
|        | LDA     | 0.21 $\pm$ 0.11                 | 0.20 $\pm$ 0.11                 | 0.20 $\pm$ 0.10                 | <b>0.17<math>\pm</math>0.08</b> |
|        | SVM     | 0.23 $\pm$ 0.11                 | 0.37 $\pm$ 0.25                 | 0.33 $\pm$ 0.23                 | 0.34 $\pm$ 0.23                 |
|        | AZT     | <b>0.02<math>\pm</math>0.01</b> | <b>0.08<math>\pm</math>0.06</b> | <b>0.16<math>\pm</math>0.09</b> | 0.27 $\pm$ 0.01                 |
| Data 2 | Binary  | 0.36 $\pm$ 0.26                 | 0.36 $\pm$ 0.25                 | 0.33 $\pm$ 0.20                 | 0.31 $\pm$ 0.18                 |
|        | k-Means | 0.28 $\pm$ 0.11                 | 0.33 $\pm$ 0.10                 | 0.33 $\pm$ 0.07                 | 0.30 $\pm$ 0.08                 |
|        | LDA     | <b>0.19<math>\pm</math>0.12</b> | 0.20 $\pm$ 0.13                 | 0.11 $\pm$ 0.11                 | 0.18 $\pm$ 0.08                 |
|        | SVM     | 0.48 $\pm$ 0.20                 | 0.45 $\pm$ 0.23                 | 0.46 $\pm$ 0.21                 | 0.48 $\pm$ 0.23                 |
|        | AZT     | 0.22 $\pm$ 0.22                 | <b>0.16<math>\pm</math>0.07</b> | <b>0.11<math>\pm</math>0.05</b> | <b>0.16<math>\pm</math>0.11</b> |

### 4 DISCUSSION

The results illustrated in figures 1 and 2, show that AZT outperforms the other algorithms in terms of sensitivity (for small segments), while generally offering the smallest specificity. This is an attractive property for the clinical automatic scanning, when it is more important not to miss a seizure, although more false positives (FP) are introduced. While LDA, k-Means and SVM give stable results for different segments' length, the AZT tended to have lower sensitivity for longer segments. AZT also

showed smaller standard deviation for the true positive (TP) rate than the other methods, and the nearest pair of TP/FP to those defined by the optimal cut-off of the ROCs in average (Table 1). This means that the implicit thresholding in AZT offers a better compromise of sensitivity and specificity.

One important limitation of the procedure followed here is that blind one-component PARAFAC decomposition may not always extract the epileptic activity. We tested that when this step was supervised to ensure using the correct component as the spatio-spectral pattern, the classification results with AZT improved in the worst cases (Table 3). This procedure is much slower and implies training the clinician in the correct use of the PARAFAC model.

Table 3: Classification results for one 2-s long seizure pattern of Data 2. A) Using blind one-component PARAFAC. B) Using one PARAFAC component (out of 3) that best characterized the seizure.

| Method       | A) Sen       | Spe          | B) Sen       | Spe          |
|--------------|--------------|--------------|--------------|--------------|
| Binary       | <b>0.963</b> | <b>0.898</b> | 1.000        | 0.362        |
| k-Means      | 1.000        | 0.751        | 1.000        | 0.806        |
| LDA (linear) | 0.838        | 0.976        | 0.813        | 0.991        |
| SVM (linear) | 0.438        | 0.999        | 0.688        | 0.999        |
| AZT          | 0.963        | 0.518        | <b>0.938</b> | <b>0.941</b> |

In summary, the uniqueness of the PARAFAC decomposition ensures the subject-specific characterization of seizures as well as the natural cleaning of the data by screening only for the activity of interest. The analysis exposed here corresponds to a segment by segment detection with just one pattern seizure, which can be done online and with low computational burden. The feature extracted via one-component blind PARAFAC is a good descriptor of pattern seizure (AUC>.97) and the proposed adaptive zero-training (AZT) online classification technique is a promising method for fast unsupervised seizure detection. Better results can be expected with visual selection of the epileptic component by a specialist. Finally, a more complete validation of this methodology is necessary in a larger epilepsy EEG database.

### REFERENCES

- Miwakeichi F, Martínez-Montes E et al. (2004) Decomposing EEG data into Space-Time-Frequency Components using Parallel Factor Analysis. *Neuroimage* 22: 1035-1045.
- Martínez-Montes, E., Márquez-Boccalandro, Y., et al. (2013). EEG Pattern Recognition by Multidimensional

Space-Time-Frequency Analysis. In *V Latin American Congress on Biomedical Engineering CLAIB 2011 May 16-21, 2011, Habana, Cuba* (pp. 1150-1153).

Orosco, L., Correa, A. G., and Lacia, E. (2013). Review: A Survey of Performance and Techniques for Automatic Epilepsy Detection. *Journal of Medical and Biological Engineering*, 33(6), 526-537.

